DOI: 10.1002/ejic.200800388

Synthesis, Structure, Spectroscopic Studies and Magnetic Properties of the Tetrakis(5,7-dichloro-8-quinolinolato)gadolinium(III) Complex

Flavia Artizzu,[a] Kevin Bernot,[b,c] Andrea Caneschi,[b] Eugenio Coronado,[d] Juan M. Clemente-Juan,[d] Luciano Marchiò,[e] Maria Laura Mercuri,[a] Luca Pilia,[a] Angela Serpe,[a] and Paola Deplano*[a]

Keywords: Gadolinium / N,O ligands / Magnetic properties / Spectroscopy

The synthesis and structural characterization of the neutral gadolinium tetrakis-type complex with 5,7-dichloro-8-quinolinolato (H5,7ClQ) ligands, $[Gd(5,7ClQ)_2(H5,7ClQ)_2Cl]$, is reported. The Gd^{III} ion is epta coordinated to one chloride ion and to four ligands: two N,O-chelated monoanions and two as zwitterionic (^+NH and O^-) monodentate oxygen donors. Electronic and vibrational spectra provide suitable markers to distinguish the presence of deprotonated and protonated ligands. The magnetic behaviour of this compound was investigated and explained by taking into account that π–π stacking interactions between the (H5,7ClQ) ligands give rise to a ferromagnetic interaction between the gadolinium centres. The Gd^{III} derivatives provide magnetic evidence for the presence of stacking interactions, which are usually undetectable in optically active Er^{III} derivatives.

Introduction

Since the first report by Tang and Van Slyke[1,2] on efficient green electroluminescence (EL) from (quinolinolato)aluminium(III) (AlQ_3, Q = 8-quinolinolate), metal chelates of this ligand have been recognized as useful emitting materials for organic light-emitting devices such as OLED diodes. Emission is due to a π*–π transition of the ligand that is strongly enhanced by coordination to a metal ion. In these last years, many efforts have been made to improve the luminescence properties of this class of emitting molecules and to "finetune" the emission wavelength by varying the metal ion or the nature and the position of the substituents on the quinoline ring.[3,4]

Recently, studies have also been carried out on the luminescence properties in the near infrared region of (quinolinolato)lanthanides (Er^{III}, Nd^{III}, Yb^{III}) to investigate their possible applications as emitting materials for telecom technology and for medical imaging purposes.[5–18] In these cases, emission arises from intrashell electronic transitions between the 4f orbitals of the lanthanide ion, and the light harvesting Q ligand acts as an antenna chromophore that can allow indirect excitation of the lanthanide ion by populating its higher levels by means of an energy-transfer mechanism (sensitized emission).[8,14]

Although (quinolinolato)lanthanides represent a class of compounds that have been widely used as low-cost functional materials for several technological applications, no reliable structural or spectroscopic analysis was available in the literature until recently, and these reports involve the interpretation of experimental results on the basis of the common assumption of a lanthanide mononuclear structure with octahedral coordination geometry.[5–16] A reinvestigation of the preparation of (quinolinolato)erbium compounds has been recently performed by us[19,20] and by the Van Deun group[17] to point out the conditions to obtain well-defined pure products as required for photophysical studies and applications. It has been shown that the reaction between an erbium halide and HQ in the presence of ammonia does not produce the invoked octahedral ErQ_3 but rather a trinuclear Er_3Q_9 complex, where each metal reaches octa coordination.[19] In the case of the 5,7-dihalo-8-quinolinolato ligands, mononuclear tetrakis complexes, where the ion is coordinated to four ligands (two deprotonated chelating, two as zwitterionic monodentate oxygen donors) and one halide, are obtained in organic solvents without the addition of a base. The full characterization of these

[a] Dipartimento di Chimica Inorganica ed Analitica, Università di Cagliari,
Cittadella di Monserrato, 09042 Monserrato, Cagliari, Italy
E-mail: deplano@unica.it
[b] Laboratory of Molecular Magnetism, Dipartimento di Chimica e UdR INSTM di Firenze, Polo Scientifico,
Via della Lastruccia 3, 50019 Sesto Fiorentino, Fi, Italy
[c] Sciences Chimiques de Rennes, UMR 6226 CNRS-INSA Rennes, Equipe Matériaux Inorganiques: Chimie Douce et Réactivité, INSA Rennes,
20 Avenue des Buttes de Coësmes, CS 14315, 35043 Rennes Cedex, France
[d] Instituto de Ciencia Molecular (ICMol), Universidad de Valencia,
C/ Dr. Moliner 50, 46100 Burjasot, Spain
[e] Dipartimento di Chimica Generale ed Inorganica, Chimica Analitica, Chimica Fisica,
Parco Area delle Scienze 17A, 43100 Parma, Italy
Supporting information for this article is available on the WWW under http://www.eurjic.org or from the author.

complexes allows the photophysical behaviour of these complexes to be explained by a structure–property relationship.[19,20] We are extending these studies to gadolinium complexes to check whether or not similar products are obtained on varying the lanthanides and to find reliable spectroscopic markers in the structurally characterized samples that can be used as diagnostic tools to distinguish different coordination modes of the ligands. Moreover, the gadolinium complexes are useful compounds to be used as a reference for a deeper understanding of magnetic and photophysical properties of the class of lanthanide quinolinolato complexes.[8,21,22] In fact, the Gd^{III} ion, with a $^8S_{7/2}$ ground term, has, contrary to the other lanthanides, no orbital contribution to the magnetic moment and the Heisenberg–Dirac–Van Vleck Hamiltonian can be employed to quantify the magnetic exchange interaction in such compounds.[23] This allows weak magnetic interactions that are usually hindered by the depopulation of the Stark sublevels of the orbitally degenerated lanthanide ions (such as Er^{III}) to be found. The high spin carried by this cation makes Gd^{III}-based compounds of interest for several biomedical applications, in particular as MRI contrast agents.[24]

We report here the synthesis, structure, full electronic and vibrational spectroscopic data and magnetic behaviour of a neutral gadolinium tetrakis-type complex with 5,7-dichloro-8-quinolinolato (H5,7ClQ) ligands, $[Gd(5,7ClQ)_2(H5,7ClQ)_2Cl]$, where the Gd^{III} ion is coordinated to four quinolinolato ligands and a chloride ion.

Results and Discussion

Synthesis and Crystal-Structure Description

The complex $[Gd(5,7ClQ)_2(H5,7ClQ)_2Cl]$ was prepared by treating 5,7-dichloro-8-quinolinol (H5,7ClQ) with $GdCl_3{\cdot}6H_2O$ in CH_3CN/CH_3OH (4:1). Given the increased acidity of the dihalo-substituted 8-hydroxyquinolines (due to the presence of electron-withdrawing groups, especially in the 7-position of the phenoxy ring) with respect to the unsubstituted one,[25] partial ligand deprotonation immediately takes place upon addition of the Gd^{III} ion to the ligand solution to form the chelated complex without the addition of a base to deprotonate the ligand hydroxy group. The reaction mixture was then stirred under gentle heating (50–60 °C) for approximately 1 d, and the solution was carefully evaporated under reduced pressure until saturation (colour turned to orange). Well-shaped, deep-red crystals suitable for X-ray structural analysis were obtained after slow evaporation of the solvent over a few days. The crystal structure revealed that $[Gd(5,7ClQ)_2(H5,7ClQ)_2Cl]$ is isostructural with the corresponding erbium complex $[Er(5,7ClQ)_2(H5,7ClQ)_2Cl]$ previously reported,[20] and the most relevant difference is represented by the longer coordination bond lengths (≈0.1 Å) for the gadolinium complex relative to the erbium one, which is in accordance with the greater ionic radii of Gd^{III} with respect to that of Er^{III}. Selected bond lengths are reported in Table 1, and a summary of X-ray crystallographic data is reported in Table 3. The Gd ion is epta coordinated to four ligands: two N,O-chelated monoanions and two that can be formally considered as zwitterionic ligands ($^+$NH and O^-), which therefore act as monodentate oxygen donors. The charge of the metal ion is balanced by one coordinating halide (Figure 1).

Table 1. Selected bond lengths (Å) for $[Gd(5,7ClQ)_2(H5,7ClQ)_2Cl]$.

Gd1–O11	2.372(3)	Gd2–O15	2.375(3)
Gd1–O12	2.275(4)	Gd2–O16	2.271(4)
Gd1–O13	2.340(3)	Gd2–O17	2.335(4)
Gd1–O14	2.256(4)	Gd2–O18	2.250(4)
Gd1–N11	2.586(4)	Gd2–N15	2.568(4)
Gd1–N13	2.607(5)	Gd2–N17	2.599(5)
Gd1–Cl1	2.667(2)	Gd2–Cl2	2.665(2)

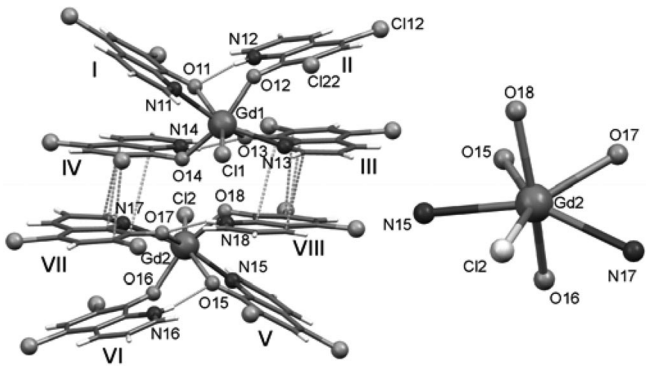

Figure 1. Molecular structure of the $[Gd(5,7ClQ)_2(H5,7ClQ)_2Cl]_2$ moiety. Dashed bonds represent intermolecular π interactions and intramolecular hydrogen bonds (left). Coordination environment of the Gd^{III} ion (right).

The coordination geometry of $[Gd(5,7ClQ)_2(H5,7ClQ)_2Cl]$ can be described as distorted pentagonal bipyramid with the equatorial positions defined by Cl1–O11–O13–N11–N13 for Gd1 and Cl2–O15–O17–N15–N17 for Gd2. The two protonated quinolines act as hydrogen-bond donors with the $^+$NH moiety, which is directed toward the oxygen atoms of the opposite, N,O-chelated quinoline. Geometric parameters of the hydrogen bonds are reported in Table 2. In the unit cell, two independent molecules are present, which are related by a pseudo centre of symmetry (Figure 1). The two independent molecules interact through a partial stack between the III–VIII and IV–VII quinoline molecules with the minimum distance between these stacks of 3.422(8) (C93···C108) and 3.439(8) Å (C97···C104). The crystal packing reveals the presence of two interconnected layers in the *ac* and *bc* crystallographic planes. These layers are determined by the partial stack of I and VI quinoline molecules (*bc* layer) and by the partial stack of the I–VI and II–V quinoline molecules (*ac* layer; Figure 2).

Table 2. Geometric parameters of the hydrogen bonds of $[Gd(5,7ClQ)_2(H5,7ClQ)_2Cl]$.

	d (Å)	N–H···X (°)
N12··O11	2.759(6)	164.5(3)
N14 ··O13	2.953(6)	162.5(3)
N16 ··O15	2.737(5)	163.4(4)
N18 ··O17	2.953(6)	161.2(3)

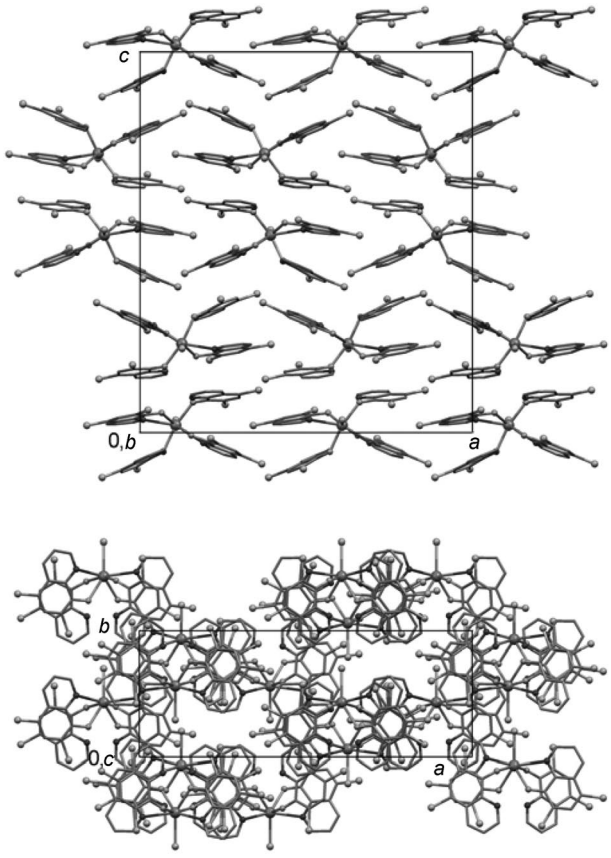

Figure 2. Crystal packing of $[Gd(5,7ClQ)_2(H5,7ClQ)_2Cl]$ projected along the *b* (above) and *c* (below) crystallographic axes.

It could be inferred that the formation of the "zwitterionic" complex from the reaction mixture under neutral conditions undergoes competitive prototropic equilibria between the different forms of the quinolinol, strongly influenced by the presence of the metal ion.[26] The tautomeric rearrangement of the neutral quinolinol in the complex is probably due to the preference of the strong Ln^{III} Lewis acid for anionic oxygen-donor atoms. No similar tetrakis complexes with the first series of lanthanides (Ce–Eu) have been obtained so far. The preparation of this kind of complex seems limited to the metals across the period from gadolinium to ytterbium (results to be published). Taking into account that the coordination chemistry of lanthanides is mostly governed by ionic bonding and steric effects, the position of gadolinium as a borderline metal between the "light" and "heavy" lanthanides[27] and related features such as the preferred coordination number, spreading from 6 to 12, may explain the observed trend.

Electronic Spectroscopy

UV/Vis absorption spectra of MeOH solutions of $[Gd(5,7ClQ)_2(H5,7ClQ)_2Cl]$ and of the free ligand both in the neutral (H5,7ClQ) and in the deprotonated form ($5,7ClQ^-$) are shown in Figure 3. The remarkable redshift in the spectrum of the quinolinolate anion with respect to that of the neutral form arises from the significant localization of the frontier orbitals on different ligand moieties, and the HOMO is mostly localized on the phenoxide ring.[3,20] The spectrum of the complex in the 300–500 nm range consists of two prominent bands. The lowest one, peaked at about 395 nm, is attributable to a π–π* ligand-centred transition and closely reflects that of the deprotonated form of the ligand. The absorption band peaked at about 340 nm is more intense and arises also from the contribution of the zwitterionic form of the quinolinolato ligand. The lowest energy f–f transition ($^8S_{7/2} \rightarrow {}^6P_{7/2}$) of the Gd^{III} ion expected at about 275 nm falls under the ligand absorption bands.[27]

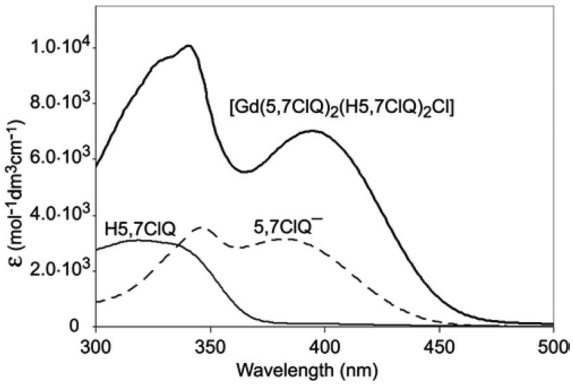

Figure 3. UV/Vis spectra of $[Gd(5,7ClQ)_2(H5,7ClQ)_2Cl]$ in MeOH solution. The spectra of the ligand are reported for comparison.

The position of the high-energy peak is modestly affected by coordination, whereas the low-energy peak is redshifted to an extent comparable to that generally observed in complexes with closed-shell metal ions.[4] This modest redshift is in agreement with the prevailing ionic character of the metal–ligand bonding.

Calculations based on semiempirical extended Hückel methods performed by using the CACAO program[29] have shown that the frontier orbitals of $[Gd(5,7ClQ)_2(H5,7ClQ)_2Cl]$ consist of a set of four closely spaced HOMOs and four LUMOs that are mostly localized on the quinolinolato ligands, whereas the contribution of the orbitals of the lanthanide ion is negligible.

As expected, the HOMO and LUMO are π orbitals of ligand character. The sketches of the last HOMO and the first LUMO (Figure 4) clearly show that each frontier orbital of the complex arises from the contribution of both the anionic and the zwitterionic form of the ligand. Moreover, the HOMO is mostly localized on the phenoxide ring of the quinolinolato ligand (with a considerable antibonding contribution of the halo substituents), whereas, for the LUMO, orbital contribution is mainly given by the pyridine ring.[3,20] This explains the charge transfer character of the π–π* ligand-centred transition that originates the lowest-energy absorption band.

In the diffuse reflectance spectrum (Figure 5) recorded on a crystalline sample of $[Gd(5,7ClQ)_2(H5,7ClQ)_2Cl]$, the peaks arising from the ligand-centred π–π* transition are slightly redshifted. This spectrum shows the same sequence

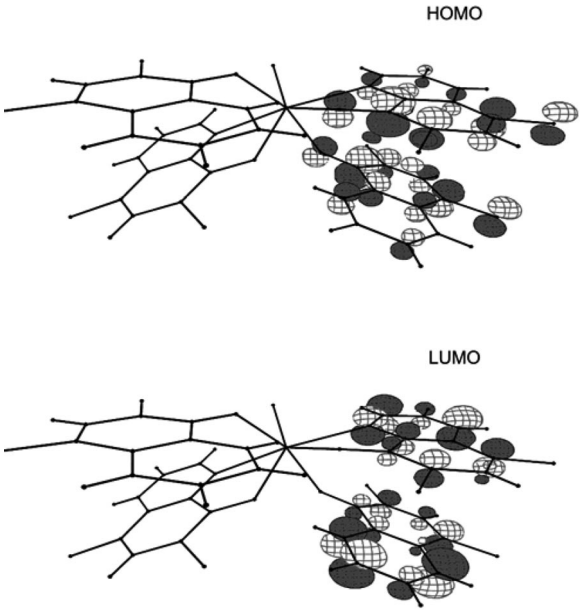

Figure 4. Frontier molecular orbitals calculated by using semiempirical extended Hückel methods through the CACAO program.

of bands as that in the solution spectrum in the UV/Vis spectral region, and an additional broad shoulder near 480 nm, which is related to solid-state effects due to the crystal-packing arrangement. According to Brinkmann et al.[30] who correlated the spectral features of different crystalline phases of AlQ_3 to the density of the packing and particularly to the π–π orbital overlap between adjacent quinoline moieties, this band could be assigned to a π–π* intermolecular transition due to π stacking, which is particularly effective in this complex (short contacts between quinoxaline rings, III–VIII and IV–VII, of adjacent molecules in the 3.4–3.8 Å range).

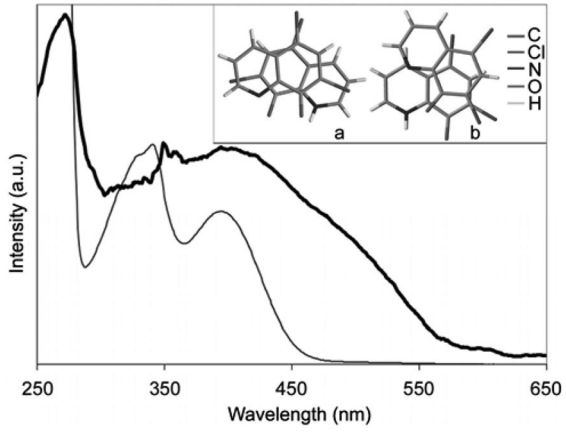

Figure 5. Diffuse reflectance spectra of $[Gd(5,7ClQ)_2(H5,7ClQ)_2Cl]$ (thick line). For comparison, the MeOH solution spectrum is also reported. In the insert a schematic drawing of the relative stack between neighbouring quinolinolato ligands in the crystal packing is reported [(a) intramolecular stacking between II and III quinolinolato rings; (b) intermolecular stacking between III–VIII ligands].

Vibrational Spectroscopy

The FTIR spectrum of $[Gd(5,7ClQ)_2(H5,7ClQ)_2Cl]$ along with the spectrum of the free ligand H5,7ClQ are reported in the Supporting Information. The spectrum is mainly dominated by aromatic ring vibrations of the quinolinolato ligand with only slight modifications due to coordination. On the basis of previous ab initio studies on AlQ_3,[31] it is possible to assign the aromatic CH vibrations near 3050 cm^{-1}, the ring stretching in the 1620–1300 cm^{-1} range and the CO stretching near 1100 cm^{-1}. This band, as well as the bands near 740 cm^{-1} (ring breathing) and near 586 cm^{-1}, are split as a consequence of the existence of two different forms of coordinated quinolinol moieties in the complex. The two bands at 957 and 879 cm^{-1} are due to CCl stretching vibrations.[8] The sequence of bands between 672 and 634 cm^{-1} is typical of this type of tetrakis(quinolinolato)lanthanide and is related to the presence of the zwitterionic ligand along with the band at 1310 cm^{-1}, whereas a weak band at about 2110 cm^{-1} is assignable to the ^+NH stretching vibration. The band near 504 cm^{-1} is likely due to the Gd–O vibration[32] or to a combination of ring vibrations and M–O stretching.[31] In the region between 3200 and 2600 cm^{-1}, another peculiar sequence of weak peaks that likely originated from combinations of the ring stretching modes is found. A similar pattern of an unresolved sequence of peaks is also found in the FT-Raman spectrum of crystalline samples. This behaviour seems characteristic of (quinolinolato)lanthanides with extensive π stacking.

Magnetic Measurements

The thermal variation in the $\chi_M T$ product is shown in Figure 6. The value of $\chi_M T$ at room temperature is close to the expected value of 7.88 emu K mol^{-1} for one isolated Gd^{III} ($S = 7/2$, $g = 2.00$).[23] The $\chi_M T$ product takes a constant value equal to 7.8 emu K mol^{-1} from 300 to 15 K. Below 15 K, the $\chi_M T$ product increases abruptly to reach a value of 8.11 emu K mol^{-1} at 2 K.

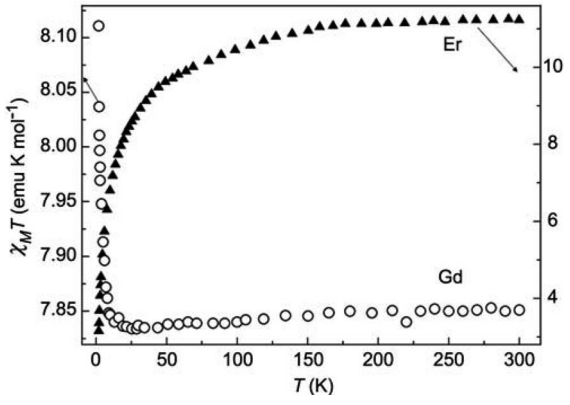

Figure 6. Temperature dependence of the $\chi_M T$ product in the temperature range 2–300 K for the Gd^{III} derivative (circles, left axis and ticks) and the Er^{III} derivative (triangles, right axis and ticks).

The experimental magnetization from 0 to 60 kOe is shown in Figure 7. The value of the magnetization at 60 kOe is 38883 emu mol^{-1} (6.96 μ_B), which is close to the expected saturated value of 7 μ_B.

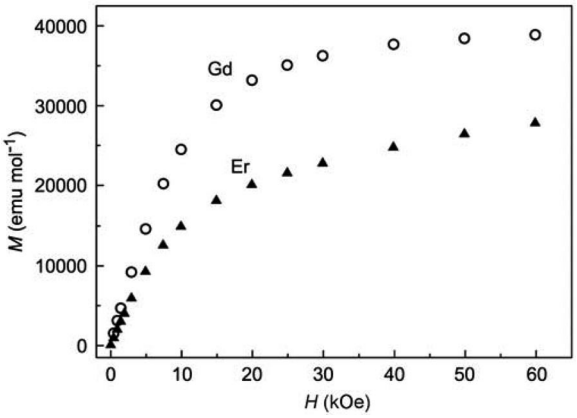

Figure 7. Field dependence of the magnetization for the Gd^{III} derivative (circles) and the Er^{III} derivative (triangles).

We can compare these magnetic measurements with the one performed on the previously reported Er^{III} derivative.[20] The corresponding $\chi_M T$ versus T curve is reported in Figure 6. At room temperature the $\chi_M T$ value (11.46 emu K mol^{-1}) is in agreement with the theoretically expected one [$\chi_M T_{(r.t.)}$ = 11.48 emu K mol^{-1}] for a Er^{III} ion ($^4I_{15/2}$, g_J = 6/5, J = 15/2). The $\chi_M T$ product takes a constant value from 300 to 150 K, and then continuously decreases when lowering the temperature to reach the value of 3.16 emu K mol^{-1} at 2 K. As expected for this type of compound, the M versus H curve does not show any saturation, and the magnetization at 60 kOe (27812 emu mol^{-1}, 4.97 μ_B) is lower than the saturated value (50265 emu mol^{-1}; see Supporting Information).

Even if these $\chi_M T$ versus T curves seem to be different they are the consequence of the same magnetic behaviour. In fact, the Gd^{III} derivative shows an increase in the $\chi_M T$ product at low temperature that is characteristic of a small ferromagnetic interaction between two Gd^{III} centres. Considering the arrangement of the [Gd(5,7ClQ)$_2$(H5,7ClQ)$_2$-Cl] moieties in the crystal structure, this small magnetic interaction is likely to be mediated by the stacking interaction through the quinoline molecules.

From a magnetic point of view, such stacking interactions are not expected to provide direct magnetic exchange interaction, but can anyway give rise to small ferromagnetic interactions between the magnetic centres.[33] Because the stacking interactions are very numerous in this crystal structure, it is almost impossible to assign which pathways is responsible for the ferromagnetic interaction visible in the $\chi_M T$ versus T curve. As the Gd^{III} is nonorbitally degenerated, a Curie–Weiss fit is usually performed in order to quantify this interaction. In our case, the interaction is so small that this procedure is affected by the noise of the measurement and consequently the fit is not reported here. This justifies again why we ascribe the rising of the $\chi_M T$ product at low temperature to a π–π interaction mediated by the (H5,7ClQ) ligands and not to a direct magnetic exchange interaction between the Gd^{III} ion (expected to be more significant).

The Er^{III} derivative is also expected to behave in the same way, as seen on numerous comparative studies along the lanthanides series.[34] The Er^{III} ion is a Kramer ion with a $^4I_{15/2}$ ground state[35] and is affected, as all the lanthanide ions that are orbitally degenerated, by a strong spin–orbit coupling. In particular, the ground state is split in Stark sublevels under the influence of the crystal field[34] (the crystal-field effects are of the order of 100 cm^{-1} for lanthanides). Consequently, when the temperature decreases, the depopulation of these sublevels leads to a deviation from the Curie law, which leads to variation in the $\chi_M T$ product, even in the absence of any exchange interaction. Below 150 K, the decrease in the $\chi_M T$ product for this compound is therefore only attributed to the depopulation of the Stark sublevels of the Er^{III} ions. The $\chi_M T$ product versus T curve can be fitted by using a simple axial zero-field Hamiltonian with D = 16.3 cm^{-1} and g = 1.2, in agreement with similar models used to fit the data of other Er^{III} complexes, for example, the double-decker bis(phthalocyaninato)lanthanide complexes.[36] Hence, the small interaction seen on the Gd^{III} derivative is expected to be also present on the Er^{III} one, as the two compounds are isostructural. However the depopulation of the Stark sublevels hampers its observation.

Even if not surprising, these magnetic measurements have confirmed the presence of significant stacking interactions through the quinoline molecules in both the Gd^{III} and Er^{III} derivatives, which are responsible for the additional band in the visible region of the diffuse reflectance spectrum.

Conclusions

A new mononuclear neutral tetrakis gadolinium complex coordinated to one chloride ion and four ligands derived from 5,7-dichloro-8-quinolinol, two deprotonated chelating and two as zwitterionic monodentate oxygen donors, was prepared in satisfactory yield and fully characterized. Electronic and vibrational spectra provide suitable markers to distinguish the presence of deprotonated and protonated ligands.

The magnetic behaviour of this compound was investigated and explained by taking into account that the π–π stacking interactions give rise to a crystal structure in which the gadolinium centres can interact ferromagnetically. In a more general picture, Gd^{III} derivatives seem to be quite efficient in providing magnetic evidence for the presence of stacking interactions, which are usually undetectable in optically active Er^{III} derivatives. We thus confirm the presence of structural interactions that are responsible for solid-state effects that influence the optical properties of the investigated compounds. In fact, the presence of significant stack-

ing interactions through the quinoline molecules has been evidenced to be at the origin of the additional band in the diffuse reflectance spectrum, and also in the redshift of the emission of the ligand.

Experimental Section

General: All the reagents and solvents were purchased from Aldrich and used without further purification. Diffuse reflectance (DR) spectra were acquired with the use of KBr pellets and absorption spectra as CH_3OH solutions (10^{-4} mol L^{-1}) and recorded with a Varian Cary 5 spectrophotometer. FTIR spectra were acquired for KBr pellets and collected with a Bruker Equinox 55 spectrophotometer. FT Raman spectra of crystalline samples were collected with a Bruker RFS/100S spectrometer operating in a back-scattering geometry with a Nd:YAG (1064 nm) laser source. C, H, N analysis was conducted with a Carlo Erba mod.EA1108 CHNS analyzer.

[Gd(5,7ClQ)$_2$(H5,7ClQ)$_2$Cl]: 5,7-Dichloro-8-quinolinol (0.412 g, 1.925 mmol) was dissolved in CH_3CN/CH_3OH (4:1, 100 mL) at 50–60 °C. A slight excess of $GdCl_3{\cdot}6H_2O$ (0.202 g, 0.543 mmol) dissolved in CH_3CN/CH_3OH (4:1, 10 mL) was slowly added to the ligand solution, and the reaction mixture turned suddenly yellow. After 24 h, the solution was concentrated under reduced pressure until it turned orange and then left to stand in air. It is important to take good care in concentrating the mother liquor in order to avoid immediate precipitation of the rather insoluble neutral 5,7-dichloro-8-quinolinol. The free ligand and the complex seem to have similar solubilities in organic solvents, thus working with a slight excess of the lanthanide ion may ensure that the crystallization of the complex takes place in advance, otherwise H5,7ClQ will be subtracted from the equilibrium and no lanthanide complex can be obtained. Any ligand residue that could precipitate after crystallization of the complex can be removed by washing with diethyl ether. After a few days red crystals, suitable for X-ray studies, were collected and washed with diethyl ether (yield 0.452 g, 45%). FTIR: $\tilde{\nu}$ = 3236 (vw), 3171 (vw), 3102 (w), 3026 (w), 2966 (w), 2914 (w), 2850 (vw), 2752 (vw), 2110 [w, $\nu(^+NH)$], 2013 (w), 1616 (m), 1592 (w), 1558 (s), 1541 (m), 1489 (m), 1452 (vs), 1393 (m), 1373 (s), 1310 (m), 1292 (w), 1250 (w), 1232 (mw), 1219 (m), 1192 (m), 1144 (m), 1111 [m (split peak)], 1051 [mw (δCH)], 991 (vw), 957 [m (νCCl)], 876 [m (νCCl)], 809 (m), 789 (m), 747 [s (split peak)], 672 (m), 658 (m), 645 (w), 634 (m), 585 (w), 572 (mw), 503 (m), 417 (mw) cm^{-1}. FT Raman: 3068 (s), 2887 (m), 1592 (s), 1574 (s), 1552 (m), 1469 (m), 1360 (vs), 1291 (mw), 1145 (m), 1051 [m (δCH)], 761 (m), 727 (m), 500 (m), 404 (m), 357 (m), 203 (m), 168 (m), 142 (m). UV/Vis (ε, mol^{-1} dm^3 cm^{-1}): λ = 340 [$(10.07 \pm 0.03) \times 10^3$], 395 [$(7.01 \pm 0.02) \times 10^3$] nm. DR (KBr): λ = 272, 358 sh., 480 sh., 410, 1667 (2νC–H) nm. $C_{36}H_{18}Cl_9GdN_4O_4$ (1046.89): calcd. C 41.30, H 1.73, N 5.35; found C 41.37, H 1.70, N 5.18.

Data Collection and Structure Determination: Single-crystal data was collected with a Bruker AXS Smart 1000 area detector diffractometer (Mo-K_α; λ = 0.71073 Å). Cell constants were obtained from a least-square refinement of selected strong reflections distributed over a hemisphere of the reciprocal space.[37] No crystal decay was observed. Absorption correction by using the SADABS[38] program was applied, which resulted in minimum and maximum transmission factors of 0.735–1.000. The structure was solved by direct methods (SIR97)[39] and refined with full-matrix least-squares (SHELXL-97)[40] by using the Wingx software package.[41] Non-hydrogen atoms were refined anisotropically. The H atoms of the protonated quinoline molecules were located from the difference Fourier map, but they were placed at their calculated positions. The remaining H atoms were placed at their calculated positions. The maximum and minimum peaks on the final difference Fourier maps corresponded to 1.396 and –0.828 e Å^{-3}. Graphical material was prepared with the ORTEP3 for Windows[42] program. A summary of the X-ray crystallographic data for [Gd(5,7ClQ)$_2$(H5,7ClQ)$_2$Cl] is presented in Table 3.

Table 3. Summary of X-ray crystallographic data for [Gd(5,7ClQ)$_2$(H5,7ClQ)$_2$Cl].

Empirical formula	$C_{72}H_{36}Cl_{18}Gd_2N_8O_8$
Formula weight	2093.69
Colour, habit	orange, prism
Crystal size (mm)	$0.45 \times 0.30 \times 0.22$
Crystal system	orthorhombic
Space group	$Pca2_1$
a (Å)	25.678(2)
b (Å)	9.771(1)
c (Å)	29.367(2)
α (°)	90
β (°)	90
γ (°)	90
V (Å^3)	7368(1)
Z	4
T (K)	293
$\rho_{calcd.}$ (Mg m^{-3})	1.887
μ (mm^{-1})	2.501
θ range (°)	1.59 to 27.99
No. of reflections/observed $F > 4\sigma(F)$	83722/13821
GooF	1.011
R_1[a]	0.0390
wR_2[b]	0.0749

[a] $R_1 = \Sigma||F_o| - |F_c||/\Sigma|F_o|$. [b] $wR_2 = \{\Sigma[w(F_o^2 - F_c^2)^2]/\Sigma[w(F_o^2)^2]\}$ 1/2, $w = 1/[\sigma^2(F_o^2) + (aP)^2 + bP]$, where $P = [\max(F_o^2,0) + 2F_c^2]/3$.

Magnetic Measurements: All magnetic measurements were performed on pellets. The *dc*-magnetic susceptibility measurements were performed with a Cryogenic S600 SQUID magnetometer between 2 and 300 K in an applied magnetic field of 1000 Oe for temperatures in the range 2–100 K and 10000 Oe for temperatures between 100 and 300 K. These measurements were all corrected for the diamagnetic contribution as calculated with Pascal's constants.

Crystallographic Data: CCDC-685127 contains the supplementary crystallographic data for this paper. These data can be obtained free of charge from The Cambridge Crystallographic Data Centre via www.ccdc.cam.ac.uk/data_request/cif.

Supporting Information (see footnote on the first page of this article): FTIR spectra of [Gd(ClQ)$_2$(HClQ)$_2$Cl] and of the H5,7ClQ ligand, χ_MT product vs. temperature plot for the Er^{III} derivative, magnetization vs. field curve at 2 and 5 K for the Er^{III} derivative.

Acknowledgments

The Fondazione Banco di Sardegna, Università di Cagliari, MIUR (PRIN-2005033820_002 "Molecular materials with magnetic, optical and electrical properties"), COST Action D35, (WG11 "Multifunctional and Switchable Molecular Materials"), EC "Network of Excellence" MAGMANet and RTN QuEMolNa (MRTN-CT2003-504880) are gratefully acknowledged for their financial support.

[1] C. W. Tang, S. A. Van Slyke, *Appl. Phys. Lett.* **1987**, *51*, 913.
[2] C. W. Tang, S. A. Van Slyke, C. H. Chen, *J. Appl. Phys.* **1989**, *65*, 3610.
[3] C. H. Chen, J. Shi, *Coord. Chem. Rev.* **1998**, *171*, 161.
[4] R. Ballardini, G. Varani, M. T. Indelli, F. Scandola, *Inorg. Chem.* **1986**, *25*, 3858.
[5] R. J. Curry, W. P. Gillin, *Appl. Phys. Lett.* **1999**, *75*, 1380.
[6] W. P. Gillin, R. J. Curry, *Appl. Phys. Lett.* **1999**, *74*, 798.
[7] Khreis, R. J. Curry, M. Somerton, W. P. Gillin, *J. Appl. Phys.* **2000**, *88*, 777.
[8] M. Iwamuro, T. Adachi, Y. Wada, T. Kitamura, S. Yanagida, *Chem. Lett.* **1999**, 539.
[9] M. Iwamuro, T. Adachi, Y. Wada, T. Kitamura, N. Nakashima, S. Yanagida, *Bull. Chem. Soc. Jpn.* **2000**, *73*, 1359.
[10] Khreis, W. P. Gillin, M. Somerton, R. J. Curry, *Org. Electron.* **2001**, *2*, 45.
[11] S. W. Magennis, A. J. Ferguson, T. Bryden, T. S. Jones, A. Beeby, I. D. W. Samuel, *Synth. Met.* **2003**, *138*, 463.
[12] R. J. Curry, W. P. Gillin, *Synth. Met.* **2000**, *111–112*, 35.
[13] R. J. Curry, W. P. Gillin, A. P. Knights, R. Gwilliam, *Opt. Mater.* **2001**, *17*, 161.
[14] J. Thompson, R. I. R. Blyth, G. Gigli, R. Cingolani, *Adv. Funct. Mater.* **2004**, *14*, 979; R. I. R. Blyth, J. Thompson, Y. Zou, R. Fink, E. Umbach, G. Gigli, R. Cingolani, *Synth. Met.* **2003**, *139*, 207.
[15] Y. Li, H. Yang, Z. He, L. Liu, W. Wang, F. Li, L. Xu, *J. Mater. Res.* **2005**, *20*, 2940.
[16] S. Penna, A. Reale, R. Pizzoferrato, G. M. Tosi Beleffi, D. Musella, W. P. Gillin, *Appl. Phys. Lett.* **2007**, *91*, 021106.
[17] R. Van Deun, P. Fias, K. Driesen, K. Binnemans, C. Görller-Walrand, *Phys. Chem. Chem. Phys.* **2003**, *5*, 2754–2757; R. Van Deun, P. Fias, P. Nockemann, A. Schepers, T. N. Parac-Vogt, K. Van Hecke, L. Van Meervelt, K. Binnemans, *Inorg. Chem.* **2004**, *43*, 8461.
[18] S. Comby, D. Imbert, A.-S. Chauvin, J.-C. G. Bünzli, *Inorg. Chem.* **2006**, *45*, 732.
[19] F. Artizzu, P. Deplano, L. Marchiò, M. L. Mercuri, L. Pilia, A. Serpe, F. Quochi, R. Orrù, F. Cordella, F. Meinardi, R. Tubino, A. Mura, G. Bongiovanni, *Inorg. Chem.* **2005**, *44*, 840.
[20] F. Artizzu, P. Deplano, L. Marchiò, M. L. Mercuri, L. Pilia, A. Serpe, F. Quochi, R. Orrù, F. Cordella, M. Saba, A. Mura, G. Bongiovanni, *Adv. Funct. Mater.* **2007**, *17*, 2365.
[21] G. A. Crosby, R. E. Whan, R. M. Alire, *J. Chem. Phys.* **1961**, *34*, 743.
[22] M. L. Bhaumik, M. A. El-Sayed, *J. Phys. Chem.* **1965**, *69*, 275.
[23] O. Kahn, *Molecular Magnetism*, Wiley-VCH, Weinheim, **1993**.
[24] P. Caravan, J. J. Ellison, T. J. McMurry, R. B. Lauffer, *Chem. Rev.* **1999**, *99*, 2293–2352 and references cited therein; V. W.-W. Yam, K. K.-W. Lo, *Coord. Chem. Rev.* **1999**, *184*, 157.
[25] H. Gershon, M. W. McNeil, S. G. Shulman, J. W. Parkes, *Anal. Chim. Acta* **1972**, *62*, 43–47.
[26] F. Goldman, E. L. Wehry, *Anal. Chem.* **1970**, *42*, 1178.
[27] R. H. Byrne, B. Li, *Geochim. Cosmochim. Acta* **1995**, *22*, 4575.
[28] J.-C. G. Bunzli, C. Piguet, *Chem. Soc. Rev.* **2005**, *34*, 1048.
[29] C. Mealli, D. Proserpio, *J. Chem. Educ.* **1990**, *67*, 39.
[30] M. Brinkmann, G. Gadret, M. Muccini, C. Taliani, N. Masciocchi, A. Sironi, *J. Am. Chem. Soc.* **2000**, *122*, 5147; H. Kaji, Y. Kusaka, G. Onoyama, F. Horii, *J. Am. Chem. Soc.* **2006**, *128*, 4292.
[31] M. D. Halls, R. Aroca, *Can. J. Chem.* **1998**, *76*, 1726.
[32] H. F. Aly, F. M. Abdel Kerim, A. T. Kandil, *J. Inorg. Nucl. Chem.* **1971**, *33*, 4340–4344.
[33] G. Novitchi, S. Shova, A. Caneschi, J.-P. Costes, M. Gdaniec, N. Stanica, *Dalton Trans.* **2004**, 1194.
[34] C. Benelli, D. Gatteschi, *Chem. Rev.* **2002**, *102*, 2369 and references cited therein.
[35] R. L. Carlin, *Magnetochemistry*, Springer, Berlin, **1986**, p. 228.
[36] N. Ishikawa, M. Sugita, T. Okubo, N. Tanaka, T. Iino, Y. Kaizu, *Inorg. Chem.* **2003**, *42*, 2440.
[37] *SMART (control) and SAINT (integration) software for CCD systems*, Bruker AXS, Madison, WI, USA, **1994**.
[38] *Area-Detector Absorption Correction*; Siemens Industrial Automation, Inc., Madison, WI, USA, **1996**.
[39] A. Altomare, M. C. Burla, M. Camalli, G. L. Cascarano, C. Giacovazzo, A. Guagliardi, A. G. G. Moliterni, G. Polidori, R. Spagna, *J. Appl. Crystallogr.* **1999**, *32*, 115.
[40] G. M. Sheldrick, *SHELX97: Programs for Crystal Structure Analysis* (release 97–2), **1997**, University of Göttingen, Germany.
[41] L. J. Farrugia, *J. Appl. Crystallogr.* **1999**, *32*, 837.
[42] L. J. Farrugia, *J. Appl. Crystallogr.* **1997**, *30*, 565.

Received: April 16, 2008
Published Online: July 9, 2008

